Electronic Supplementary Material (ESI) for New Journal of Chemistry.

Nitrogen and phosphorus enriched pyridine bridged inorganic-organic hybrid material for supercapacitor application

Nisha Dhiman and Paritosh Mohanty*

Functional Materials Laboratory, Department of Chemistry, Indian Institute of Technology Roorkee, Roorkee, Uttarakhand-247667, India

*E-mail: pmfcy@iitr.ac.in, paritosh75@gmail.com

Phone: +91-1332-284859, Fax: +91-1332-286202

Characterization of HPHM

The structural characterization of HPHM was carried out using FT-IR, NMR, XPS and XRD. The FT-IR spectra were recorded on Perkin Elmer spectrum 2 spectrophotometer. The ^{13}C and ^{31}P cross polarization magic angle spinning (CP-MAS) NMR spectra, and ^{13}C and ^{31}P NMR spectra of the precursors were taken using JEOL resonance JNM-ECX-400II spectrophotometer. The XPS of HPHM has been carried out using PHI 5000 Versa Probe III. The XRD pattern of the specimen was obtained using Bruker D8 FOCUS X-ray diffractometer with Cu K_α radiation (λ= 1.5405 Å) at a scanning speed of 4° min^{-1} in the 2θ range of 10-80 degree. The FESEM images of the HPHM was recorded on Zeiss Ultra Plus (Carl Zeiss) with an operating voltage of 20 kV. The TEM images were obtained using TECNAIG^{2}S-TWIN microscope. The

thermogravimetric analysis (TGA) was carried out in air using EXSTAR TG/DTA6300 at 10 °C min^{-1} heating rate. The specific surface area (SA_{BET}) was estimated using N_2 sorption analysis (Autosorb iQ_2, Quantachrome instruments, USA).

The electrochemical experiments such as cyclic voltammetry (CV), galvanostatic charge-discharge (GCD) and electrochemical impedance spectroscopy (EIS) were performed using a Multi Autolab/M204 electrochemical workstation (Metrohm Autolab B.V., Netherlands). A three-electrode assembly with graphite sheet based electrode of 1 cm^2 dimension as working electrode, Pt wire as counter electrode and double junction silver/silver chloride (Ag/AgCl) electrode as reference electrode[S1-S5], was used. For the preparation of the graphite sheet based working electrode, in the first step a slurry was prepared by using active material (HPHM, 70 wt %), conducting carbon (Super P, Alfa Aesar, India, 15 wt %), and polyvinylidenefluoride (PVDF, Alfa Aesar, India, 15 wt %) in N-methylpyrrolidone (NMP, Himedia, India).[S6,S7] In order to make the slurry uniform, the slurry mixture was stirred in a magnetic stirrer for 48 h at 20 °C. The working electrodes with uniform film, different mass loading were prepared by coating the slurry on graphite sheet and dried over night at 80 °C and further, used for the electrochemical studies. To optimize the optimal mass of active material, the synthesized electrodes were employed for electrochemical measurements; CV, GCD by sweeping supercapacitor electrode between potential range of -0.7 to + 0.3 V in 0.5 N KOH and the EIS has been done at 10 mV in frequency range of 0.1 Hz to 1 kHz. Further, the solid state symmetric supercapacitor device was fabricated using PVA-KOH as electrolyte, Whatman filter paper as separator and active material with mass loading of 2.37 mg was coated on graphite sheet of 3 cm^2 dimension. The electrodes were dipped for 5 minutes in PVA-KOH gel, further assembled to make solid

state symmetric device to lit up the LEDs. The areal (C_{ar}) and specific (C_{sp}) capacitance of the electrodes from CV measurement were calculated by using eqn (S1a and S1b).

$$C_{ar} = \frac{\int I\Delta V}{v \times \Delta V \times A} \quad \text{(S1a)}$$

$$C_{sp} = \frac{\int I\Delta V}{v \times \Delta V \times m} \quad \text{(S1b)}$$

Specific capacitance from GCD was calculated using the eqn (S2):

$$C_{sp} = \left(\frac{I}{m}\right) \times \frac{\Delta t}{\Delta V - IR} \quad \text{(S2)}$$

Energy and power densities were calculated by employing eqn (S3) and (S4), respectively,

$$E = \frac{1}{2} \times C_{sp} \times \Delta V^2 \left(\frac{1000}{3600}\right) \quad \text{(S3)}$$

$$P = \frac{E}{\Delta t} \times 3600 \quad \text{(S4)}$$

where, I is response current in ampere, $^{\Delta}$V is the potential window (V), *v* is scan rate (mV s^{-1}), m (g), and A (cm^2) is the mass and area of active material respectively, Δt is the discharge time in sec, E (Wh kg^{-1}) and P (W kg^{-1}) energy and power density respectively.[S6,S7]

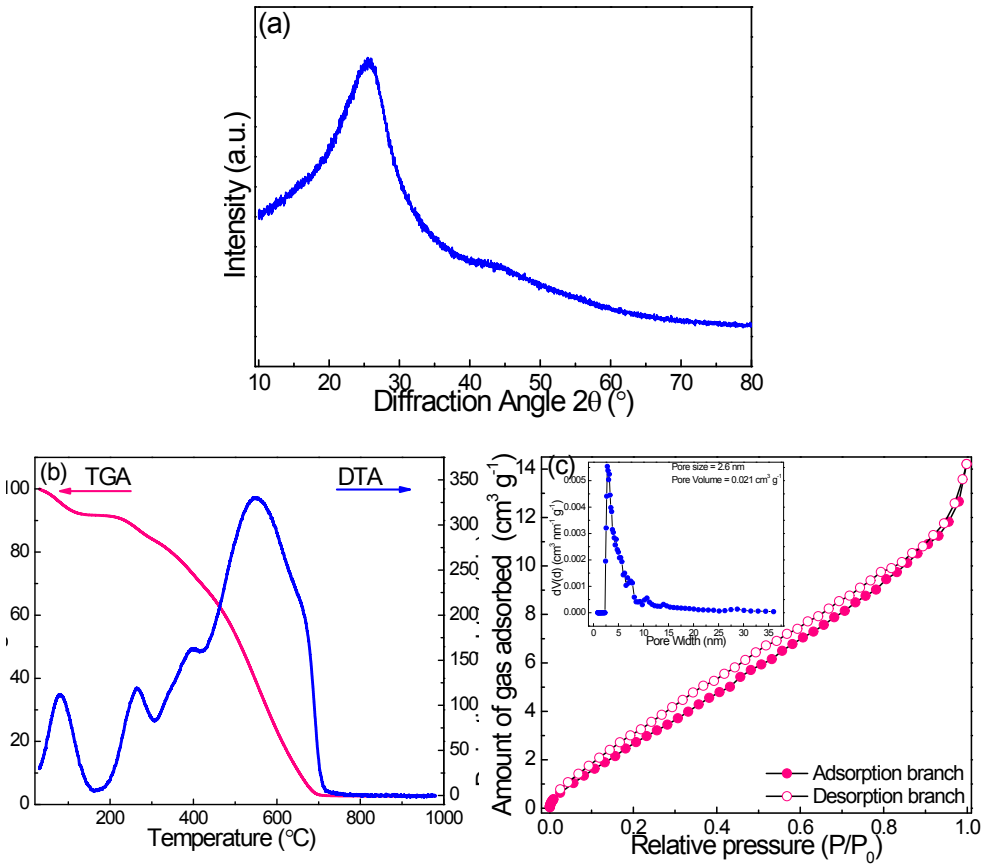

Fig. S1 (a) XRD (b) TGA and (c) N_2 sorption isotherm (inset pore size distribution) of HPHM.

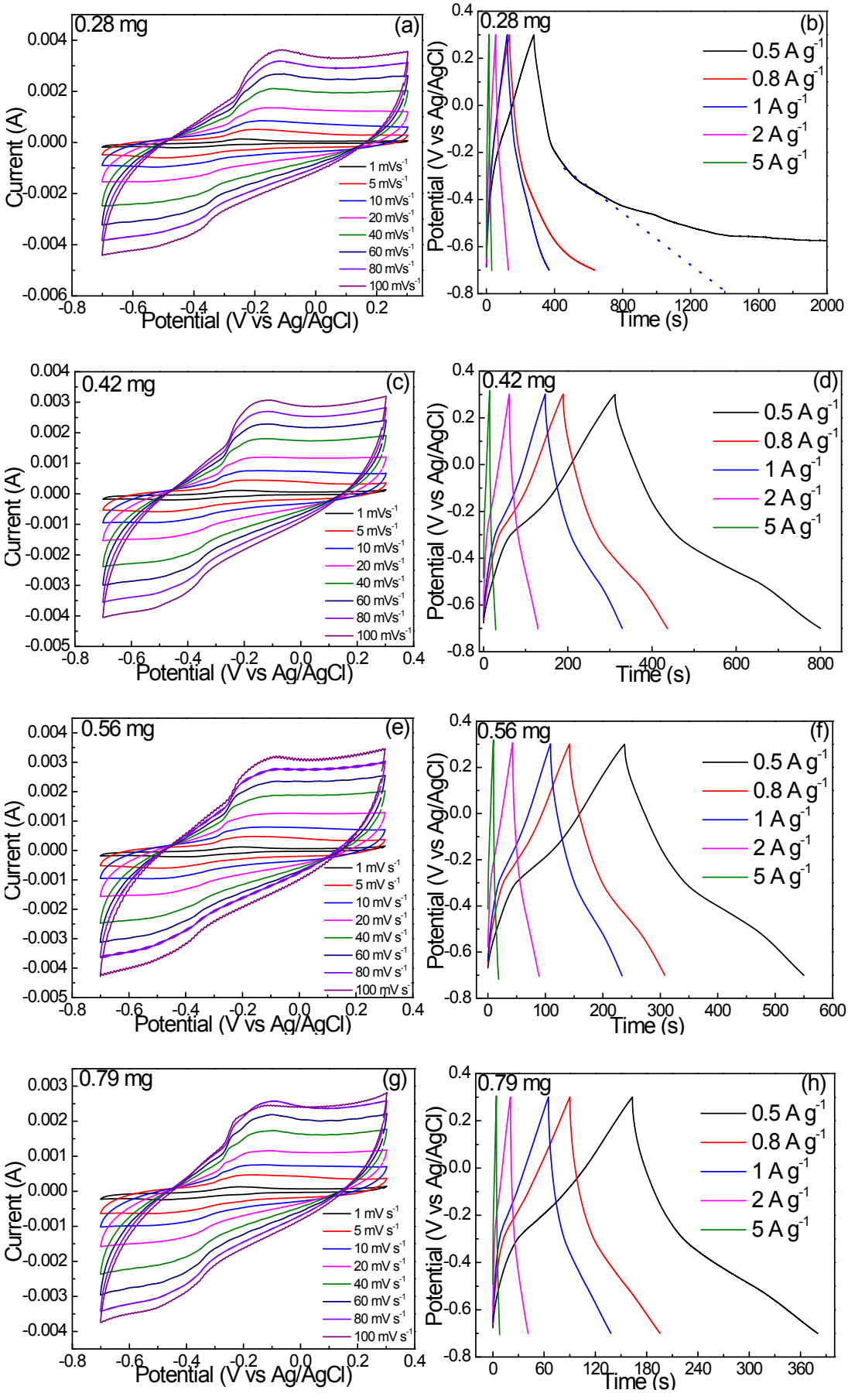
0.28 mg
(a)
Current (A)
Potential (V vs Ag/AgCl)
1 mVs-1
5 mVs-1
10 mVs-1
20 mVs-1
40 mVs-1
60 mVs-1
80 mVs-1
100 mVs-1
0.28 mg
(b)
Potential (V vs Ag/AgCl)
Time (s)
0.5 A g-1
0.8 A g-1
1 A g-1
2 A g-1
5 A g-1
0.42 mg
(c)
Current (A)
Potential (V vs Ag/AgCl)
1 mVs-1
5 mVs-1
10 mVs-1
20 mVs-1
40 mVs-1
60 mVs-1
80 mVs-1
100 mVs-1
0.42 mg
(d)
Potential (V vs Ag/AgCl)
Time (s)
0.5 A g-1
0.8 A g-1
1 A g-1
2 A g-1
5 A g-1
0.56 mg
(e)
Current (A)
Potential (V vs Ag/AgCl)
1 mV s-1
5 mV s-1
10 mV s-1
20 mV s-1
40 mV s-1
60 mV s-1
80 mV s-1
100 mV s-1
0.56 mg
(f)
Potential (V vs Ag/AgCl)
Time (s)
0.5 A g-1
0.8 A g-1
1 A g-1
2 A g-1
5 A g-1
0.79 mg
(g)
Current (A)
Potential (V vs Ag/AgCl)
1 mV s-1
5 mV s-1
10 mV s-1
20 mV s-1
40 mV s-1
60 mV s-1
80 mV s-1
100 mV s-1
0.79 mg
(h)
Potential (V vs Ag/AgCl)
Time (s)
0.5 A g-1
0.8 A g-1
1 A g-1
2 A g-1
5 A g-1

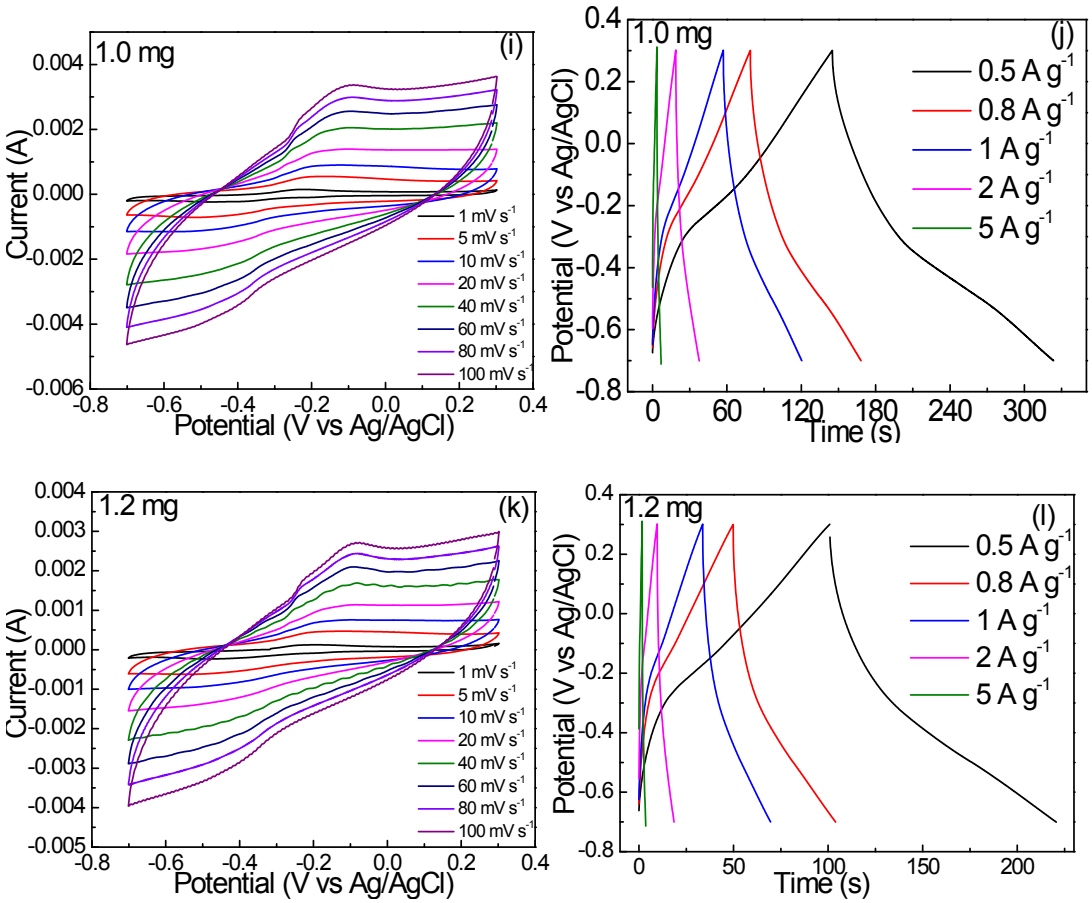

Fig. S2 CV (a, c, e, g, i and k) and GCD (b, d, f, h, j and l) of HPHM supercapacitor electrodes at different mass loading.

Table. S1a Specific capacitance values calculated from CV

S. No	Scan Rate (mV s^{-1}) / Active Mass (mg)	Specific Capacitance (F g^{-1}) from CV							
		1	5	10	20	40	60	80	100
1	**0.28**	555	424	357	303	241	202	183	167
2	**0.42**	390	287	238	190	148	123	107	97
3	**0.56**	312	224	196	151	116	95	82	75
4	**0.79**	243	163	126	101	72	61	53	45
5	**1.0**	192	144	120	95	50	50	51	46
6	**1.2**	158	110	83	62	41	38	31	25

Table. S1b Specific capacitance values calculated from GCD

S. No	Current Density (A g^{-1}) / Active Mass (mg)	Specific Capacitance (F g^{-1}) from GCD				
		0.5	**0.8**	**1**	**2**	**5**
1	**0.28**	556	407	258	144	81
2	**0.42**	243	198	184	132	70
3	**0.56**	156	132	127	90	38
4	**0.79**	107	83	73	41	18
5	**1.0**	89	72	63	38	17
6	**1.2**	60	42	36	17	6

Table. S1c Areal capacitance values calculated form CV

S. No	Scan Rate (mV s^{-1}) / Active Mass (mg)	Areal Capacitance (mF cm^{-2}) from CV							
		1	**5**	**10**	**20**	**40**	**60**	**80**	**100**
1	**0.28**	155	118	100	85	67	56	51	47
2	**0.42**	163	120	100	80	62	51	45	41
3	**0.56**	175	125	110	85	65	53	46	42
4	**0.79**	192	129	100	80	57	48	42	36
5	**1.0**	192	144	120	95	50	50	51	46
6	**1.2**	190	132	100	75	50	46	37	30

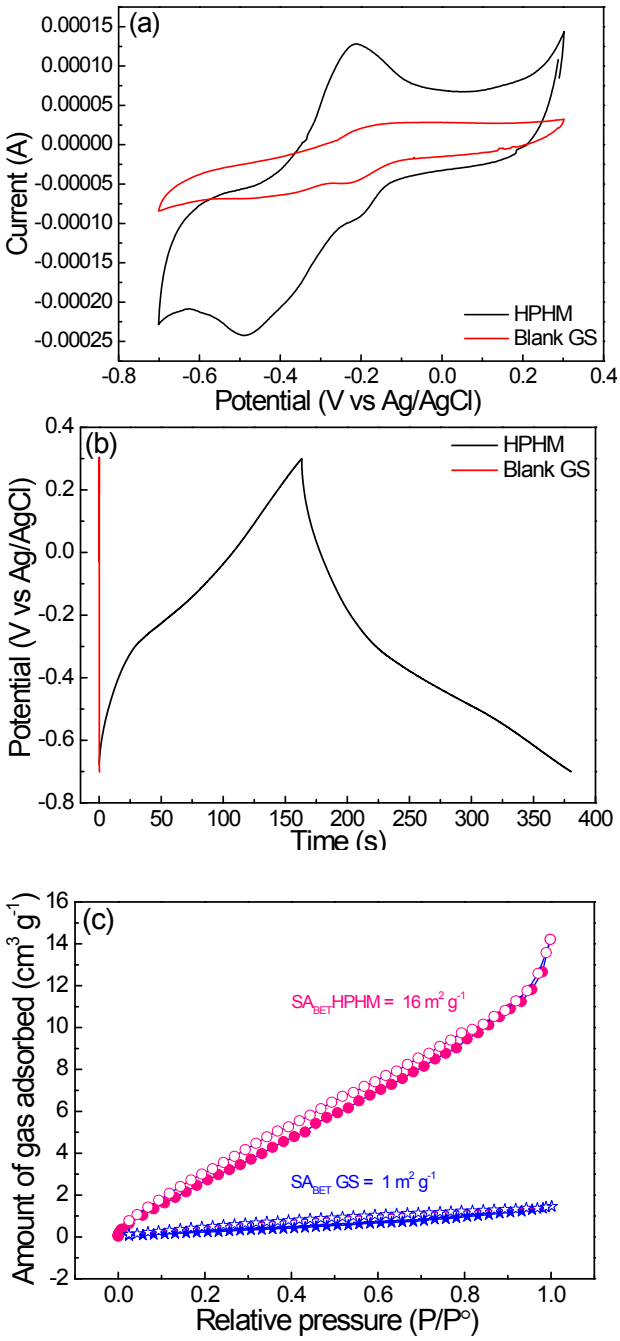

Fig. S3 Comparison of between HPHM and current collector graphite sheet (GS) (a) Cyclic voltammograms at 1 mV s^{-1} (b) Galvanostatic charge/discharge at 0.5 A g^{-1} and (c) SA_{BET}

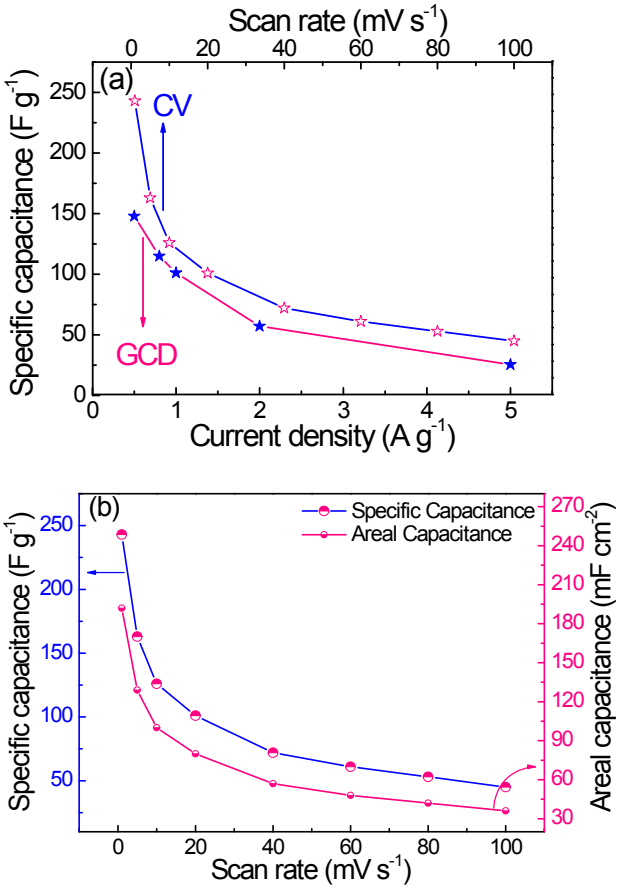

Fig. S4 (a) Comparison of specific capacitance vs current density and scan rate and (b) Comparison of specific and areal capacitance at different scan at optimal mass loading of HPHM.

Table. S2 Comparison of HPHM electrode capacitance with recent reported hybrid material.

S. N.	Hybrid Materials	C_{sp} (F g^{-1})	C_{ar} (mFcm^{-2})	Electrolyte	SA_{BET} (m^2 g^{-1})	% Retention	Ref.
1	DAP-RGO	317	--	1 M H_2SO_4	33	90	S8
2	WSS	--	5.23	1 M $LiClO_4$	--	94	S9
3	NOMCs	193	--	6 M KOH	583-847	90	S10
4	DAC@MoS_2	261	--	1 M Na_2SO_4	1509	88	S11
5	PCs	295	--	6 M KOH	1945	100	S12
6	PEDOT/PANi hydrogel	112	242	PVA-H_2SO_4	--	80.8	S13
7	Functionalized GO	127	--	--	--	90	S14
8	N,P-CBC	118	--	6 M KOH	731	76	S15
9	PEDOT NW		413	PVA-Polydopaamine- H_2SO_4	--	94	S16
10	PEDOT:PSS/MWCNT	1314	--	KI-1 M H_2SO_4	--	87.6	S17
11	PEDOT	203	--	1 M H_2SO_4	--	86	S18
12	PEDOT:PSS/MWCNT	22,3	--	PVA/H_3PO_4	--	72	S19
13	BP	80.7		PVA/H_3PO_4	--	80	S20
14	PU	43	--	PVA/H_3PO_4	--	72	S21
15	**HPHM* (*= Optimal mass loading)**	**243**	**192**	**0.5 N KOH**	**16**	**87**	**Present work**

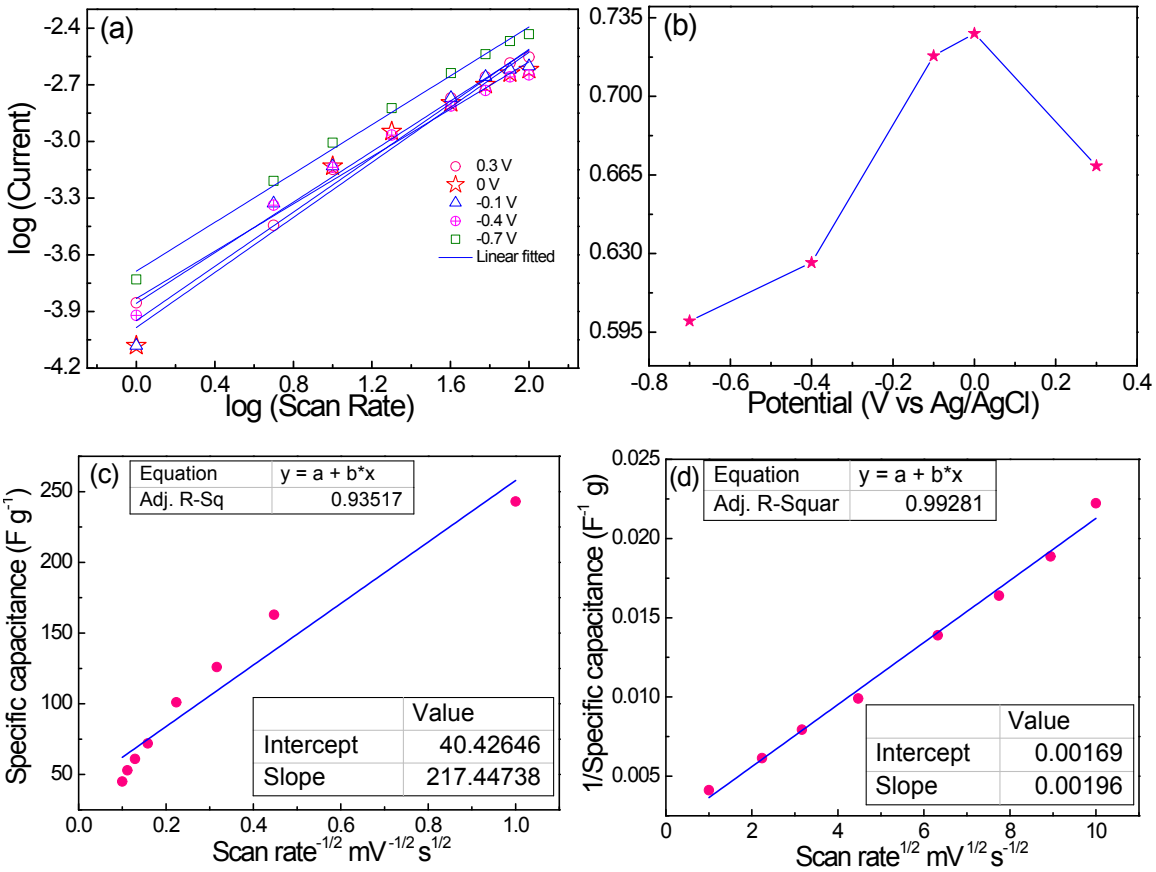

Fig. S5 EDLC and pseudo contribution calculation using (a) log (Current) vs log (Scan rate) at fixed potential (b) b values vs potential (Ag/AgCl) and (c, d) Trasatti plots.

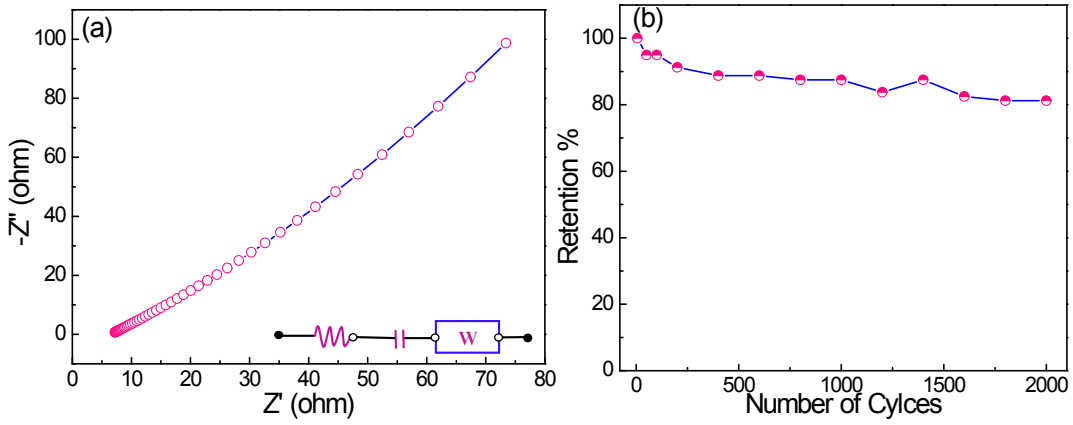

Fig. S6 (a) EIS study (equivalent circuit diagram in the inset) and (b) Cyclic stability upto 2000 cycles in 0.5 N KOH electrolyte vs Ag/AgCl.

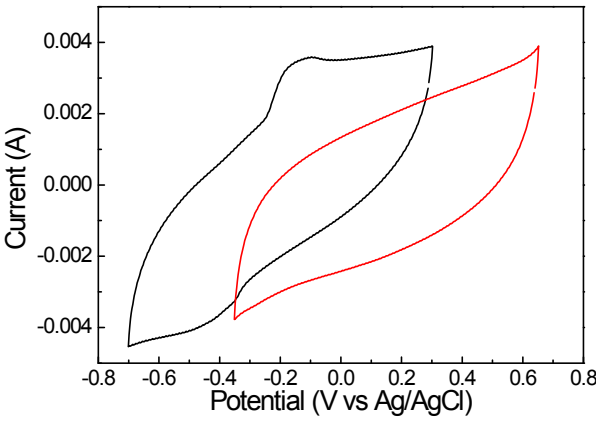

Fig. S7 Anodic and cathodic response of HPHM.

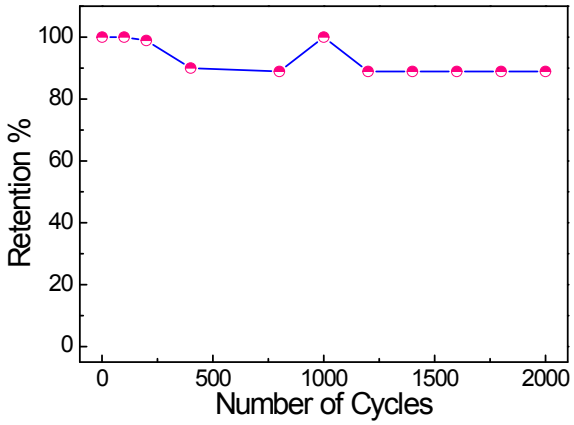

Fig. S8 Cyclic stability of HPHM solid state symmetric device upto 2000 cycles in PVA-KOH electrolyte.

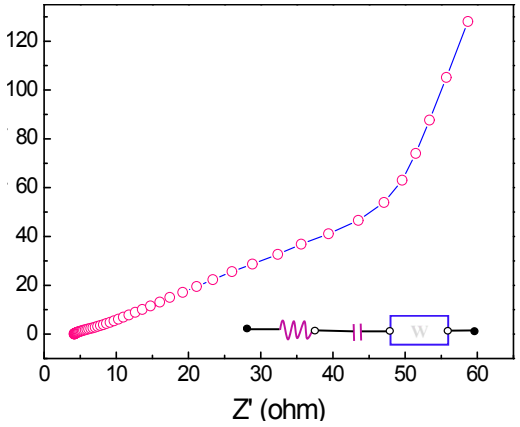

Fig. S9 EIS study (equivalent circuit diagram in the inset) of HPHM solid state symmetric device.

References

S1 C. Haider, Electrodes in potentiometry. https://www.metrohm.com/en-us/documents/80155013

S2 Silver/silver chloride reference electrode-the ecological alternative for calomel reference electrodes. https://www.metrohm.com/en/documents/81095022

S3 Q. Lu, Z. J. Mellinger, W. Wang, W. Li, Y. Chen, J. G. Chen and J. Q. Xiao, *ChemSusChem,* 2011, **3**, 1367-1370.

S4 D. Wang, A. Wei, L. Tian, A. Mensah, D. Li, Y. Xu and Q. Wei, *Appl. Surf. Sci.,* 2019, **483**, 593-600.

S5 A. S. Rajpurohit, N. S. Punde, C. R. Rawool and A. K. Srivastava, *Chem. Eng. J.*, 2019, **371**, 679-692.

S6 V. Sharma, S. Khilari, D. Pradhan and P. Mohanty, *RSC Adv*., 2016, **6**, 56421-56428.

S7 V. Sharma, A. Sahoo, Y. Sharma and P. Mohanty, *RSC Adv*., 2015, **5**, 45749-45754.

S8 X. Zhang, D. Wang, M. Yang, X. Xia, H. Chen, Y. Chen and H. Liu, *J. Solid State Electr.,* 2018, **22**, 1921-1931.

S9 K. Keum, G. Lee, H. Lee, J. Yun, H. Park, S. Y. Hong, C. Song, J. W. Kim and J. S. Ha, *ACS Appl. Mater. Interfaces,* 2018, **10**, 26248-26257.

S10 L. Liu, S. D. Xu, F. Y. Wang, Y. J. Song, J. Liu, Z. M. Gao and Z. Y. Yuan, *RSC Adv*., 2017, **7**, 12524-12533.

S11 D. N. Sangeetha and M. Selvakumar, *Appl. Surf. Sci*., 2018, **453**, 132-140.

S12 B. Chen, W. Wu, C. Li, Y. Wang, Y. Zhang, L. Fu, Y. Zhu, L. Zhang and Y. Wu, *Sci. Rep.,* 2019, doi.org/10.1038/s41598-019-41769-y.

S13 Z. Yang, J. Ma, B. Bai, A. Qiu, D. Losic, D. Shi and M. Chen, Electrochim. Acta, 2019, **322**, 134769-134778.

S14 X. Zhang, L. Hou, F. Richard and P. Samori, Chem. Euro. J., 2018, 10.1002/chem.201803184.

S15 D. Kong, L. Cao, Z. Fang, F. Lai, Z. Lin, P. Zhang and W. Li, Ionics, 2019, **25**, 4341- 4350.

S16 D. Ni, Y. Chen, H. Song, C. Liu, X. Yang and K. Cai, J. Mater. Chem. A, 2019, **7**, 1323–1333.

S17 X. Gao, L. Zu, X. Cai, C. Li, H. Lian, Y. Liu, X. Wang and X. Cui, Nanomater., 2018, **8**, doi:10.3390/nano8050335.

S18 M. Rajesh, C. J. Raj, R. Manikandan, B. C. Kim, S. Y. Park and K. H. Yu, Mater. Today Energy, 2017, **6**, 96-104.

S19 M. dos S. Klem, R. M. Morais, R. J. G. Rubira and N. Alves, Thin Solid Films, 2019, **669** 96-102.

S20 M. Wen, D. Liu, Y. Kang, J. Wang, H. Huang, J. Li, P. K. Chu and X. F. Yu, *Mater. Horiz.,* 2019, **6**, 176-181.

S21 H. T. Jeong, J. F. Du, Y. R. Kim, C. J. Raj and B. C. Kim, J. Alloy Compd., 2019, **777**, 67-72.